Biochimica et Biophysica Acta 1827 (2013) 974–985

Contents lists available at SciVerse ScienceDirect

Biochimica et Biophysica Acta

journal homepage: www.elsevier.com/locate/bbabio

Review

Molecular basis of [FeFe]-hydrogenase function ☆
An insight into the complex interplay between protein and catalytic cofactor

Martin Winkler [1], Julian Esselborn [1], Thomas Happe *

Ruhr-Universität Bochum, Fakultät für Biologie und Biotechnologie, Lehrstuhl für Biochemie der Pflanzen, AG Photobiotechnologie, 44780 Bochum, Germany

ARTICLE INFO

Article history:
Received 18 October 2012
Received in revised form 21 February 2013
Accepted 8 March 2013
Available online 16 March 2013

Keywords:
[FeFe]-hydrogenase
Ferredoxin
Green algae
Clostridium
Oxygen sensitivity

ABSTRACT

The precise electrochemical features of metal cofactors that convey the functions of redox enzymes are essentially determined by the specific interaction pattern between cofactor and enclosing protein environment. However, while biophysical techniques allow a detailed understanding of the features characterizing the cofactor itself, knowledge about the contribution of the protein part is much harder to obtain. [FeFe]-hydrogenases are an interesting class of enzymes that catalyze both, H_2 oxidation and the reduction of protons to molecular hydrogen with significant efficiency. The active site of these proteins consists of an unusual prosthetic group (H-cluster) with six iron and six sulfur atoms. While H-cluster architecture and catalytic states during the different steps of H_2 turnover have been thoroughly investigated during the last 20 years, possible functional contributions from the polypeptide framework were only assumed according to the level of conservancy and X-ray structure analyses. Due to the recent development of simpler and more efficient expression systems the role of single amino acids can now be experimentally investigated. This article summarizes, compares and categorizes the results of recent investigations based on site directed and random mutagenesis according to their informative value about structure function relationships in [FeFe]-hydrogenases. This article is part of a Special Issue entitled: Metals in Bioenergetics and Biomimetics Systems.

1. Introduction

The catalytic activity of redox enzymes often depends on metal cofactors tightly embedded in a specific polypeptide scaffold. While both parts equally contribute to catalytic functionality the characterization of metalloenzymes like e.g. hydrogenases is still primarily focused on the catalytic cofactor.

Concerning cofactor architecture the three phylogenetically unrelated hydrogenase families share the basic concept of a central Fe ion coordinated and influenced by highly unusual diatomic ligands like CO and at least concerning the two mayor families of [NiFe]- and [FeFe] hydrogeanases, CN^- [1]. [Fe]-hydrogenases, which are exclusively found in methanogenic archaebacteria, contain a single Fe ion, which is part of an organometallic compound used for H_2 dependent reduction of 5,10-methylenetetrahydromethanopterin during methanogenesis [2]. In [NiFe]-hydrogenases the Fe core element belongs to a characteristic bimetallic [NiFe]-center [3]. In the case of [FeFe]-hydrogenases the catalytically important Fe-atom represents one half of a unique and nearly symmetric diiron-moiety covalently attached to a [4Fe4S]-cluster [4,5]. The combination of classic cubane [FeS]- and unique diiron-cluster is termed H-cluster. [FeFe]-hydrogenases achieve very high production rates of up to 9000 molecules H_2 s^{-1}. This renders them highly interesting candidates concerning the establishment of applications based on bio-hydrogen or semi-artificial H_2 production systems [6].

In the last decade crystal structure analysis and X-ray absorption spectroscopy revealed the general cofactor architecture of [FeFe]-hydrogenases [4,5,7,8]. EPR, Mössbauer and IR-spectroscopy enabled the monitoring of state specific redox potentials, spin states and ligand configurations during the catalytic cycle [9–16]. On the basis of such data organometallic mimic structures of [NiFe]- and [FeFe]-cofactors are designed in growing number and diversity that again inspire and enrich basic research on architecture and catalytic function of both cofactors [17]. But only a small number of these chemical compounds exhibit significant proton reduction activity over a time range exceeding a few hours [18]. Their restricted catalytic activity indicates that the role of the polypeptide environment for the catalytic process has been underestimated.

The polypeptide environment isolates the catalytic cofactor from the solvent and provides a second ligand sphere, which might significantly influence the electrochemical features of the cofactor. A

Abbreviations: ADT, azadithiolate; CpI, [FeFe]-hydrogenase 1 from *Clostridium pasteurianum*; DdH, periplasmic [FeFe]-hydrogenase from *Desulfovibrio desulfuricans*; DFT, density functional theory; $HydA1_{Cr}$, [FeFe]-hydrogenase HydA1 from *Chlamydomonas reinhardtii*; $HydA_{Ca}$, hydrogenase 1 from *Clostridium acetobutylicum*; HYSCORE, hyperfine sublevel correlation spectroscopy; MD, molecular dynamics; MM, molecular mechanics; QM, quantum mechanics

☆ This article is part of a Special Issue entitled: Metals in Bioenergetics and Biomimetics Systems.

* Corresponding author. Tel.: +49 234 32 27026; fax: +49 234 32 14322.
E-mail address: thomas.happe@rub.de (T. Happe).

[1] Both authors contributed equally to this article.

0005-2728/$ – see front matter © 2013 Elsevier B.V. All rights reserved.
http://dx.doi.org/10.1016/j.bbabio.2013.03.004

network of iron sulfur clusters transfers electrons to and from the active site and influences the redox behavior of the H-cluster. The protein surface determines redox partner selectivity and the polypeptide structure provides selective access- and exit pathways for substrates and products. These aspects also influence O_2 sensitivity, one of the major problems to face for utilizing [FeFe]-hydrogenases.

A pre-condition for the successful design of efficient and durable bio-inspired mimics is thus a fundamental understanding of the subtle direct and indirect influences of the polypeptide chain on cofactor function. But site directed mutagenesis, the key discipline for characterizing structure function relationships in proteins has long been out of reach for [FeFe]-hydrogenase research. As researchers only recently started to identify and understand the highly specified maturation system behind H-cluster synthesis [19–24] early heterologous systems for the active expression of [FeFe]-hydrogenase variants have been rare and inefficient [19]. Two major strategies have been successfully followed to increase holoprotein yield. First, expression hosts were chosen that exhibit native [FeFe]-hydrogenase activity and thus already provide the required maturation system like *Clostridium acetobutylicum* [25,26] and *Shewanella oneidensis* [27]. On the other hand, owing to the increasing knowledge about the maturation process, standard systems based on *Escherichia coli* have been optimized for the heterologous coexpression of hydrogenase apoprotein and the three H-cluster maturases HydE, F and G [28,29].

Accordingly, during the last five years new data stepwise fill the gaps of knowledge about the partaking of conserved amino acid residues in different aspects of the turnover process. On the basis of an extensive conservancy analysis of the available [FeFe]-hydrogenase polypeptide sequence pool the present review summarizes and re-evaluates these experimental results concerning their implications for different conserved and specific structure function relationships in the [FeFe]-hydrogenase family.

2. Phylogenetic and structural diversity of [FeFe] hydrogenases

While [NiFe]-hydrogenases can be found in all major phyla of the prokaryota, [FeFe]-hydrogenase distribution is focused on the classes of δ-Proteobacteria, Clostridia and Thermotogae [30]. [FeFe]-hydrogenases are also identified among the eukaryota including several amitochondriate, anaerobic protists, where they are either localized in the cytosol (Giardia, Entamoeba) or take part in the hydrogenosomal metabolism (Trichomonads, Neocallimastix, Pyromyces, Nyctotherus) [31–35]. In green algae they are part of the complex anaerobic metabolism of the algal chloroplast and allow a coupling of light induced H_2O splitting and H_2 production [36].

The majority of [FeFe]-hydrogenases features a monomeric organization, thereby contrasting with the basically dimeric structure concept of [NiFe]-hydrogenases.

The common denominator of all [FeFe]-hydrogenases is the 40 kDa H-domain that embeds the H-cluster via four cysteinate groups in a conserved binding site characterized by three polypeptide sequence motifs (P1–P3 in Fig. 1) [37]. The smallest identified [FeFe]-hydrogenase (M1) is reduced to this catalytic core unit and has only been found in Chlorophycean green algae yet (Fig. 1) [30].

Other [FeFe]-hydrogenase monomers show a high degree of modularity by featuring up to three additional N-terminal and up to two further C-terminal cluster binding motifs containing accessory FeS clusters that mediate electron transfer between the H-cluster and redox partners of the hydrogenase (Fig. 1). Structure type M2 is characterized by an N-terminal F-domain that resembles bacterial type ferredoxins and correspondingly accommodates two additional cubane clusters. This subtype shows the highest level of distribution as it can be found in all major lineages of [FeFe]-hydrogenase phylogeny and is thus discussed as being the ancestral [FeFe]-hydrogenase group [30]. The DdH of *Desulfovibrio desulfuricans* represents a dimeric example of this structure type and has been characterized by crystal structure analysis (Fig. 1). In the course of eukaryogenesis an inactive phylogenetic sister group of the M2-[FeFe]-hydrogenase lineage addressed as NarF-like (nuclear prelamine A recognition factor) proteins has lost hydrogenase activity while being established as an essential factor for cytosolic FeS protein maturation in higher eukaryotic cells [38–41]. Subtype M3, which is typical for clostridial enzymes like CpI (Fig. 1), comprises two further N-terminal cluster binding motifs. One of these harbors a [4Fe4S]-cluster ligated by three cysteinate groups and one histidyl residue, while the other one exhibits homology to plant type ferredoxins and contains a [2Fe2S]-cluster.

When NAD(P)H/NAD(P)-turnover is coupled to H_2/H^+-turnover, an additional C-terminal domain is included that shows homology to domains of respiratory complex I (NADH-ubiquinone-oxidoreductase). These are represented either by a single thioredoxin-like [2Fe2S]-cluster domain corresponding to NuoE (M4) or consist of a NuoE-like domain and an additional [4Fe4S]-cluster motif corresponding to NuoF (M5)[31,42]. Especially subtypes M3 and M4 can be part of trimeric (Clostridia, Thermotogales) and tetrameric (δ-Proteobacteria) enzymes. Multiple forms with different modular structures are especially abundant in members of the genus *Clostridium* [43].

To create a broader base for the analysis of conserved residues and motifs, a new collection of [FeFe]-hydrogenase sequences was established (Table 1 and S1) making use of the growing number of available sequences. Using the H-domain of the CpI and $HydA1_{Cr}$ polypeptides as bait in two extended BLAST searches [44] against NCBI's database of non-redundant protein sequences, the 1000 best hits of each search were pooled and purged of redundancy. This primary pool of 1082 sequences was trimmed to 828 by excluding NarF-like sequences and sequences missing one of the conserved motifs P1–P3 (Fig. 1) or the conserved motif APav. The sequences were aligned by the MUSCLE algorithm [45] and assigned to the subtypes by the presence of accessory FeS clusters and conserved domains from NCBI's CDD database [46] (for further information see Supplementary information S1). The resulting sequences cover all major organismal lineages known as carriers of the [FeFe]-hydrogenase phenotype and exhibit a structural variance that goes beyond the established M-type structural classification (Table 1).

3. H-cluster and catalytic cycle

As introduced above the H-cluster of [FeFe]-hydrogenases consists of two coupled subclusters, a standard [4Fe4S] cubane ($4Fe_H$) and the catalytic [2Fe2S] moiety ($2Fe_H$). The two Fe-atoms (proximal Fe_p and distal Fe_d relative to $4Fe_H$) of the latter are further coordinated by highly unusual ligand molecules including two terminally bound CN^-, two to three terminally bound CO groups and in certain redox states a μ-CO group in the bridging position between both Fe atoms [4,5,7,8,47,48]. Several H-bond contacts to the CN^--ligands stabilize the general orientation of the $2Fe_H$-site within the protein environment (see below). The CO ligands are less firmly attached and switch between different configuration states in the course of the catalytic process. While both ligand types in general contribute to control the spin state of the two Fe sites, recent QM/MM calculations indicate that the essential role of the CN^- ligands may lie in focusing the HOMO (Highest Occupied Molecular Orbital) at the catalytic $2Fe_H$ moiety. This e.g. adjusts the regioselectivity of protonation in the H_{red} state and allows for fast electrochemical communication between both subclusters [49]. The bridging CO ligand on the other hand seems to be crucial for the stability of the low oxidation states of the $2Fe_H$-subcluster [50]. Modulations in the electrostatic interaction pattern between the polypeptide vicinity and the CO and CN^- ligands should therefore have a strong effect on the kinetic parameters of enzymatic catalysis.

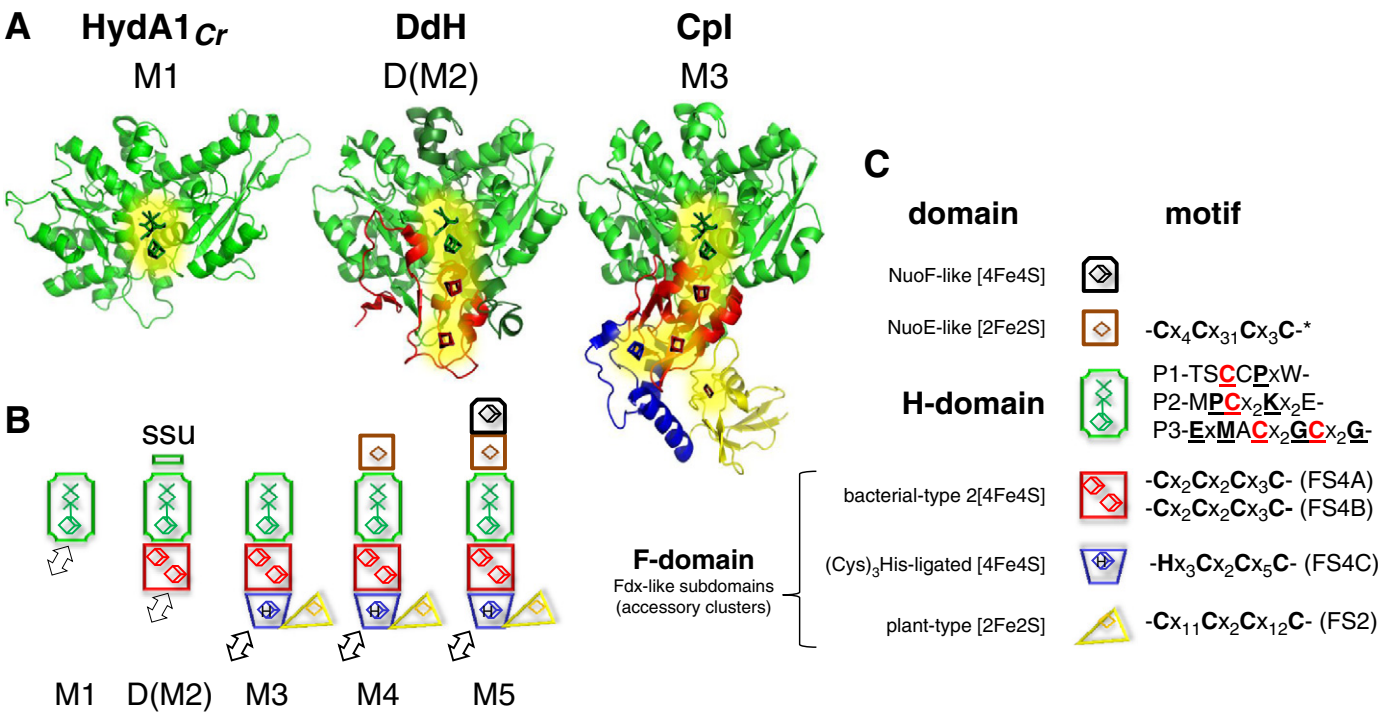

Fig 1. Structural modularity of [FeFe]-hydrogenases. Part (A) depicts ribbon-coil models of representatives of the first three [FeFe]-hydrogenase structure types (M1–3) HydA1$_{Cr}$ (PDB ID: 3LX4); DdH (PDB ID: 1HFE); CpI (PDB ID: 3C8Y). Redox cofactors participating in electron transport are indicated by stick models attributed with a yellow glow. The domain organization of the five structure types suggested by Meyer [30] is schematically presented in (B). The color code referring to both, structure models and schemes, indicates different domains in the monomeric organization, which is further explained in (C). Here for each domain cofactor content and name are presented including conserved sequence motifs, which characterize the respective domain. The sequence motifs P1-P3 of the H-domain are simplified according to [37]. H-cluster coordinating cysteines are presented in red letters. Cubes indicate [4Fe4S]-clusters while rhombs represent [2Fe2S]-clusters. Open arrows indicate putative or verified contact sites for the interaction with redox mediators. SSU: small subunit; D: dimeric hydrogenase.

The two inorganic sulfur atoms are interconnected by a dithiolate bridge whose central bridgehead atom could not be further identified on the basis of the available X-ray data [5,51]. Earlier analyses did not exclude carbon as part of a propanedithiolate group [5] while later density functional theory calculations even supported the idea of an oxadithiolate [47] bridge. However, Nicolet and coworkers soon suggested nitrogen to be the most probable candidate as the center atom of the corresponding azadithiolate (ADT) ligand ($-S-CH_2-NH-CH_2-S-$) thus yielding a secondary amine. Via Walden inversion a secondary amine could easily mediate proton transfer between the terminal position of the proton transfer pathway ($C178_{Pd}$) and the open coordination site at Fe_d without disturbing active site geometry [52]. A subsequent analysis of ^{14}N nuclear quadrupole and hyperfine interactions of the H-cluster determined by advanced EPR spectroscopy provided experimental evidence for this assumption [53].

The four cysteinates at positions 300, 355, 499 and 503 (position numbers of the enzyme CpI from *Clostridium pasteurianum*), which coordinate the Fe sites of the cubane subcluster, form the only covalent bonds between protein and H-cluster with $C503_{Cp}$ coupling the $2Fe_H$-cluster and the $4Fe_H$-cluster [4]. Apart from this bridging cysteine the catalytic di-iron center builds only non-covalent interactions between its non-protein ligands and the polypeptide environment including electrostatic contacts and a conserved H-bond network (see also Section 5; Fig. 3).

Besides stabilizing and electrochemically tuning the catalytic site, these non-covalent contacts still allow enough flexibility to enable changes in the ligand sphere configuration during the catalytic turnover process (Fig. 2). Proton-/H_2-turnover comprises two coupled electron and proton transfer steps during which the $2Fe_H$ site passes different valence distributions and ligand coordinations. In general two redox states can be spectroscopically determined as major resting states of the catalytic cycle. The paramagnetic H_{ox} state (active "oxidized") exhibits a mixed valence configuration ($4Fe_H(II)-Fe_p(I)Fe_d(II)-[\ ]/-H_2$) while the

Table 1
Distribution of sequences in the mutiple sequence alignment to subtypes.

Subtype	Number	Percentage	Selected source organisms
	Of sequences in the alignment		
M1	**10**	**1.2%**	*Chlamydomonas reinhardtii*, *Volvox carteri*, *Scenedesmus obliquus*
M2	**209**	**25.2%**	*Clostridiales*, *fusobacteria*, *Entamoeba*
M2a[a]	122	14.7%	*Desulfovibrio vulgaris* Hildenborough
M2b	30	3.6%	*Firmicutes*, *spirochetes*, *Giardia*
M2c	14	1.7%	*Firmicutes*
M2d	21	2.5%	*Firmicutes*, *fusobacteria*, *proteobacteria*
M2ARNAP[b]	14	1.7%	*Desulfo-tomaculum/-sporosinus/-vibrionales*
M2bd[c]	8	1.0%	*Clostridiaceae*
M3	**583**	**70.4%**	*Clostridium pasteurianum*, *firmicutes*, *spirochetes*, *trichomonads*, *Chlorella variabilis*
M3Flav[d]	**2**	**0.2%**	*Blastocystis hominis*, *Blastocystis* sp. NandII
M4	**22**	**2.7%**	*Thermotoga maritima*, *Spirochaeta smaragdina*, *Desulfovibrio magneticus*
M5[e]	**2**	**0.2%**	*Nyctotherus ovalis*
Total	828	100%	

[a] M2 subtype classification according to [43] if not noted otherwise.
[b] Annotated as D subunit of archaeal RNA polymerases.
[c] Contains both Acetyl-CoA-synthase bD like M2b and rubredoxin/ruberythrin domain like M2d.
[d] Annotated as containing a Flavodoxin domain.
[e] Named M5 in Meyer 2007 [30], but NuoF containing sequences could only be identified in *Nyctotherus ovalis*.

diamagnetic EPR silent H_{red} species represents the active "reduced" state assigned as $4Fe_H(II)-Fe_p(I)Fe_d(I)[H^+]$, or $4Fe_H(II)-Fe_p(II)Fe_d(II)-H^-$ in the form of a hydrido species [9–11,50,54,55].

Recently H_{sred}, a low potential redox state earlier regarded as artificial and inactive [12], has been verified as a further intermediate state in the turnover process [14,56]. Starting from H_{red} further electrochemical reduction leads to a species still exhibiting a persistent catalytic H^+-reduction current and EPR Q-band-signals characteristic for $4Fe_H(I)$. This indicates for the H_{sred} state a valence configuration of $4Fe_H(I)-Fe_p(I)Fe_d(I)[H^+]$ (Fig. 2). At least for [FeFe]-hydrogenases of structure types M2 and M3 H_{sred} seems to be a short-lived species, because the additional electron at the cubane subcluster is presumably quickly released to the chain of accessory [FeS]-clusters. As such accessory clusters are absent in M1-type enzymes like $HydA1_{Cr}$, here H_{sred} can even be trapped *in vitro* under H_2 atmosphere. According to the valence spectrum of H_{sred}, the binding site of the first proton prior to the second protonation step is still unclear. Therefore, an intermediate protonation of a nearby protein residue is suggested [56].

The active forms of the H-cluster are reversibly inhibited either by CO leading to the inactive oxidized state $H_{ox}CO$ [14,57,58] (Fig. 2) or by formaldehyde [55,59]. O_2 contact however quickly and irreversibly induces a not yet fully understood H-cluster degradation process. This process presumably starts with O_2 binding at the open coordination site of Fe_d, where it is activated and forms a reactive oxygen species (ROS). Experimental data suggest that the ROS attacks and thus destabilizes the $4Fe_H$ site prior to the loss of the $2Fe_H$ site [8,58,60] (Fig. 2). According to a complementary DFT calculation, protonation of the ROS seems to be necessary for the detached ROS (O_2^- or $OOH^\cdot$) to be thermodynamically capable to attack the $4Fe_H$-subcluster [61]. A water filled channel connecting both subclusters has been assumed, which might allow ROS translocation and protonation [61].

4. The H-cluster environment

The hydrophobic pocket, in which the H-cluster is situated, is formed by a rather complex fold of four loops and four helices [4,5]. All of them exhibit an overall high degree of conservation around the H-cluster in a multiple sequence alignment of 828 putative [FeFe]-hydrogenases (Fig. 3B).

Three of the four cysteine residues 300_{Cp}, 355_{Cp}, 499_{Cp} and 503_{Cp} coordinating the H-cluster are strictly conserved. Interestingly nearly 20% of the compared sequences feature a serine instead of $C300_{Cp}$

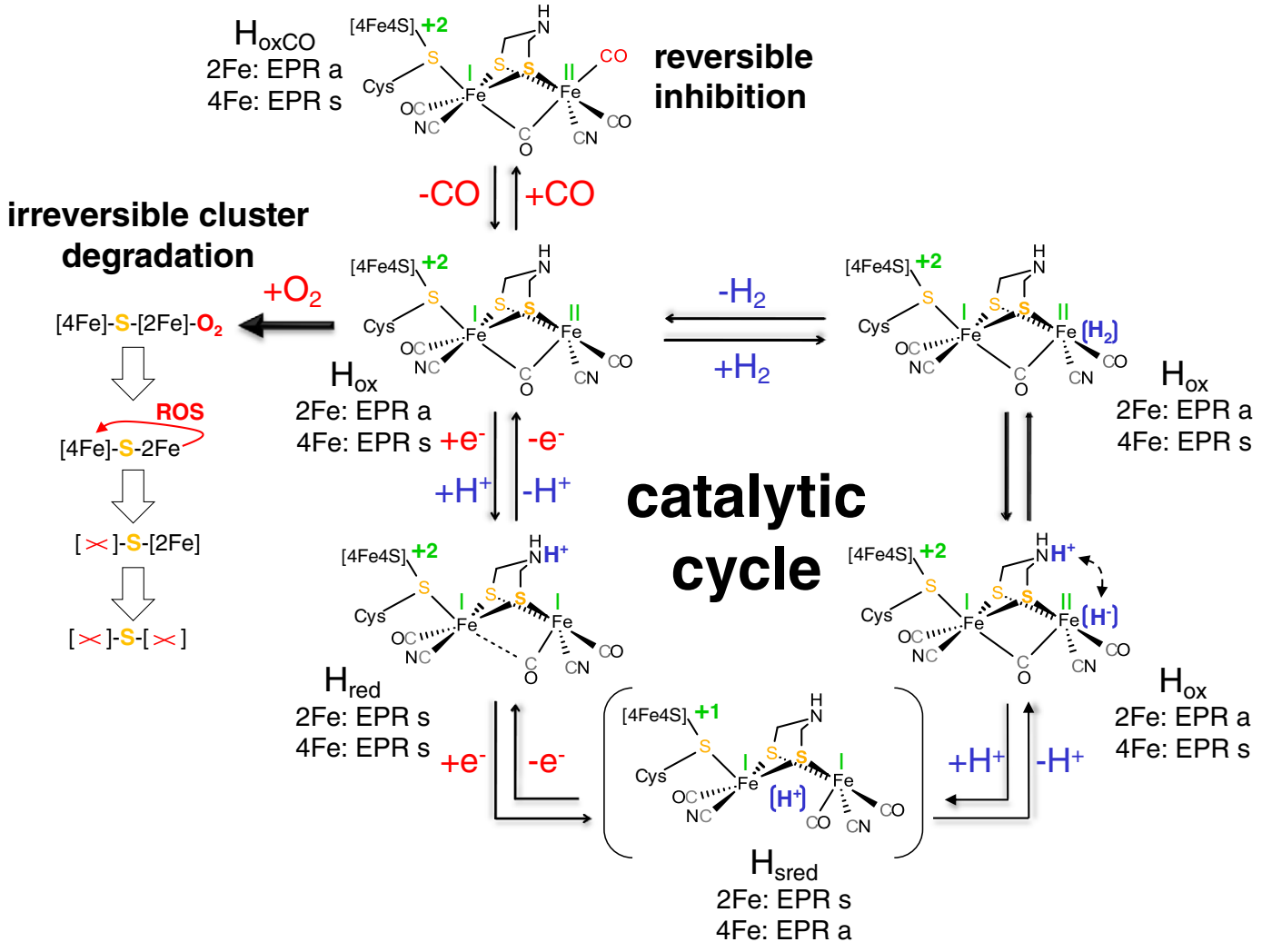

Fig. 2. Catalytic cycle of H^+ reduction and H_2 oxidation at the H-cluster of [FeFe]-hydrogenases. The presented schema is based on the mechanism proposed by Adamska and coworkers and includes the recently identified active state of H_{sred} [56]. Protonation steps, protons, hydrides and H_2 are presented in blue, reduction/oxidation steps, inhibitors (O_2, CO) and reactive oxygen species (ROS) are given in red. Valencies are added in green roman figures for the $2Fe_H$-subcluster and as green Arabian figures for the $4Fe_H$-subcluster. As the location of the proton at H_{sred} is still unclear the proton is presented in a delocalized central position in parentheses. The red bended arrow indicates the assumption of ROS translocation between the $2Fe_H$ and the $4Fe_H$ moiety after O_2-activation at $2Fe_H$. A degraded cluster part is indicated by a red cross. EPR s: EPR-silent; EPR a: EPR-active; ROS: reactive oxygen species.

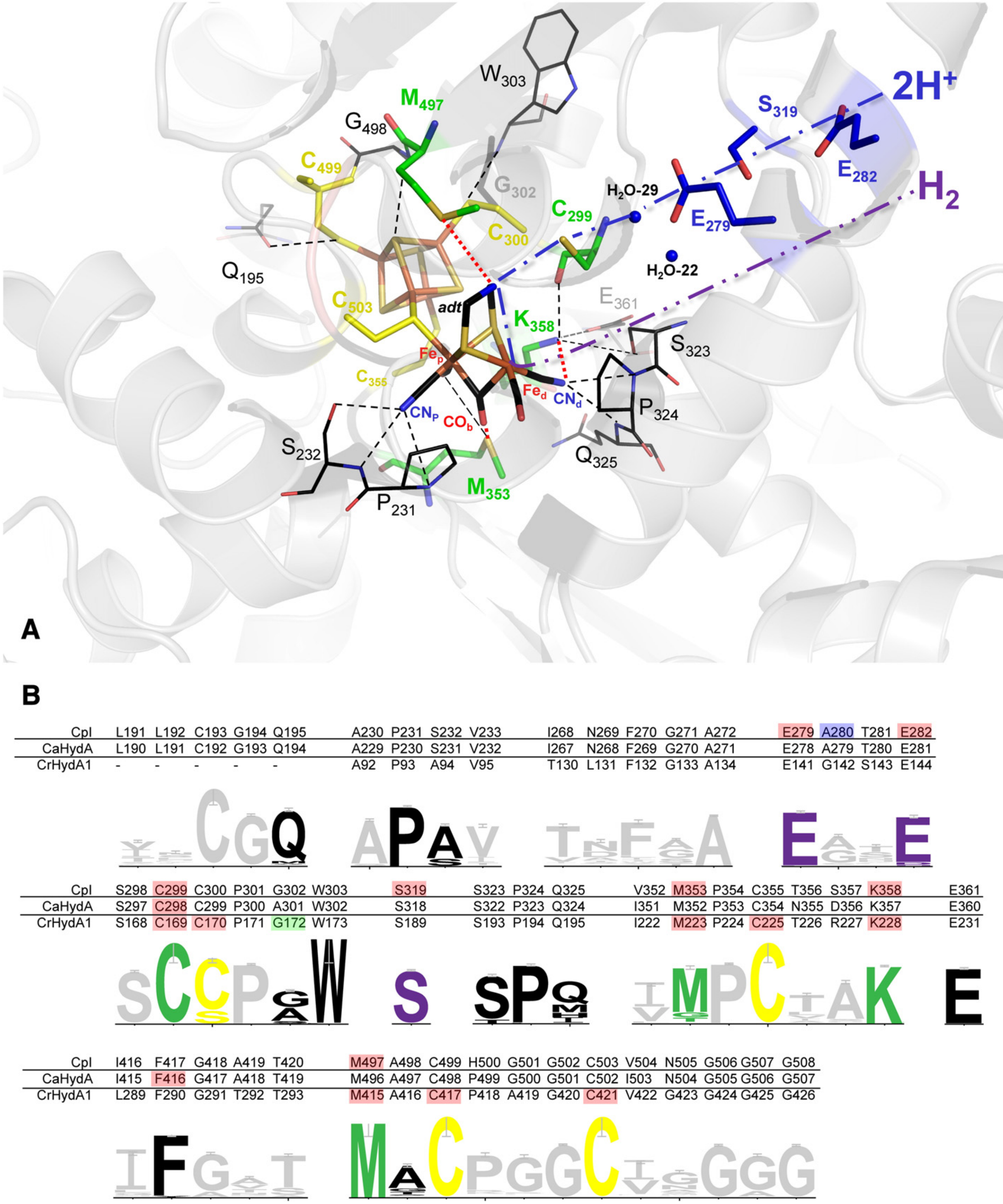

Fig. 3. H-cluster environment of CpI, alignment of sequences of the H-cluster environment and H-bond network of the $2Fe_H$ ligands. (A) Stick model representation of the H-cluster environment of CpI (PDB ID: 3C8Y) showing the H-cluster bonding cysteinates in yellow, non-covalently interacting residues in black, mutated residues in green and residues putatively forming the proton transfer pathway in blue. Interactions are indicated by dashed lines and atom-to-atom distances are presented for CpI and DdH (PDB ID: 1HFE) in Table 2. (B) Parts of the protein sequences of CpI, $HydA_{Ca}$ and $HydA1_{Cr}$ representing amino acids surrounding the H-cluster together with a sequence logo [103] of the respective positions of a multiple sequence alignment of 828 [FeFe]-hydrogenases (see Table 1 and S1). Color scheme of the sequence logo as in A. Positions in CpI, $HydA_{Ca}$ and $HydA1_{Cr}$ for which mutations affecting either catalytic activity or oxygen tolerance have been reported (see S2) are indicated by colored background: green and red background indicate positive and negative influence on catalytic activity respectively; positive and negative influence on O_2 tolerance are specified by blue and yellow background respectively.

presumably replacing the S – Fe bond by an O – Fe bond. However, when the corresponding cysteine in $HydA1_{Cr}$ ($C170_{Cr}$) is changed to serine, the activity is completely abolished. Changes of the other three cysteines similarly lead to complete loss ($C417_{Cr}$, $C421_{Cr}$) or severe decrease of activity ($C225S_{Cr}$) (Happe et al., unpublished data).

Moreover, all electrostatic interactions of the H-cluster with the immediate protein environment influence the catalytic activity. Fig. 3A depicts all residues which according to the crystal structure of CpI (PDB ID: 3C8Y, [47]) are in a position to electrostatically interact with parts of the H-cluster (black). The figure also shows residues for which results of mutagenesis studies have been reported (green stick models) and includes those believed to contribute to proton transfer between solvent and H-cluster (blue). Potential interactions of $2Fe_H$-subcluster ligands with polypeptide residues of the close protein environment are listed in Table 2 for the crystal structures of CpI and DdH (PDB ID: 1HFE, [5]) including the corresponding interatomic distances. All cofactor-interacting amino acids are strictly conserved with the exceptions of $Q325_{Cp}$ being only moderately conserved and positions $S232_{Cp}$ and $M353_{Cp}$, which still exhibit a high level of conservancy (see conservancy levels in Fig. 3B). It should be mentioned that the carbonyl oxygen of $F417_{Cp}$ potentially interacts with one of the inorganic sulfurs of the $2Fe_H$-subcluster and is also considered to be important for the maturation process [20,62].

An H-bond interaction between $K228_{Cr}$ ($K358_{Cp}$) and one of the distal diatomic groups was first suggested according to crystal structure data and led to the assignment of the distal CN^- ligand (CN^-_d) [7]. This H-bond contact was later verified by a ^{14}N-HYSCORE analysis of the DdH protein [15] and is considered to prevent the isomerization of CO and CN^--ligands at Fe_d [63]. Additionally, it seems to be important to anchor the translocated $2Fe_H$-subcluster within the open binding site of the $HydA1_{Cr}$ apoprotein during the final step of maturation [62]. Not surprisingly, the replacement of lysine at position 358 in CpI and at the homologous site 228_{Cr} by asparagine resulted in a complete loss of activity, which goes along with an incomplete H-cluster that lacks the $2Fe_H$ moiety according to EPR and FTIR analyses [64].

The central N-atom of the ADT ligand is believed to be part of the proton transfer chain between the solvent and the catalytic site at Fe_d [15,65] and is thus pivotal to the catalytic mechanism (Fig. 2). According to the available crystal structure data of CpI and DdH, the residues methionine 497_{Cp} and cysteine 299_{Cp} should be able to form NH – S or N – HS bonds with the internal amine base of the ADT bridge thereby probably modulating its basicity and proton conducting ability (Fig. 3). As expected, even conservative mutations of $C299_{Cp}$ to serine and $M497_{Cp}$ to leucine abolished or at least severely impaired the catalytic activity of CpI and $HydA1_{Cr}$ [64]. Variant $M415L_{Cr}$, corresponding to $M497_{Cp}$, was isolated as a mixture of enzyme fractions with a majority lacking the $2Fe_H$-subcluster. The minor fraction accounts for the detected residual activity of 4–5%. EPR spectroscopy revealed for the latter fraction g values that clearly deviate from the wild type spectrum, thus demonstrating that the exchange affects the electronic features and maybe even the architecture of the H-cluster [64]. Variant $C169S_{Cr}$ did quantitatively contain the complete H-cluster, however EPR and FTIR spectra of a sample expected to be in the H_{red} state instead resembled the H_{trans} state [64]. This state has been described for the [FeFe]-hydrogenase of *D. desulfuricans* upon the reversible one electron reduction of H^{air}_{ox} [10,12,66]. H_{trans} has so far not been observed for $HydA1_{Cr}$ or CpI and is characterized by a diamagnetic $2Fe_H$ and a paramagnetic $4Fe_H$-moiety with a presumed valence configuration of $4Fe_H(I) – Fe_p(II)Fe_d(II)$ [11,12] and according to DFT calculations an oxygen derived species at the open coordination site of Fe_d [50,67]. It might be speculated that the $4Fe_H(I) – Fe_p(II)Fe_d(II)$ configuration of H_{trans} represents the original state after finishing the maturation process. While wild type enzyme is quickly activated to H_{ox} the $C299S_{Cp}$ ($C169S_{Cr}$) exchange somehow arrests the H-cluster in its original state. The oxygen species at the active site might be stabilized by the serine's hydroxyl group keeping the open coordination site occupied and the enzyme in an inactive state [67]. Recent investigations on variants of $HydA_{Ca}$ indicate that it might indeed be the introduction of the hydroxyl group rather than the loss of the cysteine's thiol group, which leads to a complete loss of activity. A- and L-variants of the corresponding position C289 in the [FeFe]-hydrogenase I of *C. acetobutylicum* ($HydA_{Ca}$) show low residual H_2-uptake activity [68]. Similar effects were reported for a $C299A_{Cp}$ variant [69]. The severe loss of H_2-uptake activity and the lack of any proton reduction competence however clearly indicate a pivotal role for cysteine at position 299_{Cp} in the catalytic function presumably as H^+-donor/acceptor for the ADT ligand in proton transfer [7,69].

Recently, the screening of a saturation mutagenesis library for the corresponding position C298 of $HydA_{Ca}$ revealed that the conservative exchange to aspartic acid preserves 50% of the catalytic activity measured for wild type enzyme, while any other exchange severely diminishes enzymatic activity below the minimum detectable threshold level of 14%. The authors further confirmed the essential role of position C298 for proton transfer by demonstrating a significant shift in the pH activity profile for variant $C298D_{Ca}$ to the lower pH range [70].

According to the crystal structure of CpI the sulfur group of $M353_{Cp}$ has a distance of 3.16 Å relative to the oxygen atom of the bridging CO in position to potentially influence the behavior of this ligand (Fig. 3). However, this interaction seems not to be crucial for the structural integrity of the H-cluster as the corresponding $M223L_{Cr}$ variant displayed signals of an intact H-cluster when examined via EPR and FTIR spectroscopy albeit with subtle differences in the electronic structure and the vibrational spectra of the CO ligands [64]. Corresponding variants in both CpI and $HydA1_{Cr}$ showed strongly reduced catalytic activity. Interestingly $M223L_{Cr}$ switches to the super-reduced state much more readily than the wild type enzyme [56,64]. As indicated above, position 353_{Cp} belongs to the residues in the close H-cluster environment that are not strictly conserved. Approximately 9% of the putative [FeFe]-hydrogenase sequences analyzed here exhibit instead of a methionine a glycine and 8% a threonine at the respective position. Although it is unclear whether these minor groups of sequences encode active [FeFe]-hydrogenases, they might exhibit interesting differences in their enzymatic features.

As suggested before, according to their high conservation level and path-like orientation within the crystal structures of CpI and DdH [4,7] the residues $E279_{Cp}$, $E282_{Cp}$, $C299_{Cp}$ and $S319_{Cp}$ have recently been examined for their role in proton transfer between the solvent exposed protein surface and the active site. QM/MM MD simulations on the basis of crystal structure data for DdH and CpI complemented by first site-directed mutagenesis examinations indeed support this assumption [69,71].

Table 2
Non-covalent interactions of the $2Fe_H$-subcluster with the peptide environment.

	CpI			DdH		
ADT	C299[a]	S[b]	3.46[c]	C178	S	3.23
	M497	S	3.58	M376	S	3.91
CN_d	S323	γO	3.77	S202	γO	3.37
	P324	N	3.49	P203	N	3.62
	Q325	N	2.91	I204	N	3.1
	K358	ζN	2.87	K237	ζN	2.84
CN_p	P231	N	3.64	P108	N	3.52
	S232	N	3.13	A109	N	2.94
		γO	2.82			
CO_b	M353	S	3.16	M232	S	3.35
CO_d				T145	γO	3.94
CO_p	M353	S	3.53	M232	S	3.61
Sα	F417	O	3.44	F296	O	3.38

[a] Amino acid interacting with $2Fe_H$ ligand in the first column. Numbering as in the crystal structures 3C8Y and 1HFE.
[b] Atom of amino acid interacting with proton donor/acceptor of $2Fe_H$ ligand.
[c] Atom to atom distances in Å calculated from the structures 3C8Y and 1HFE.

Another study focused on the high-throughput screening of a randomly generated library of HydA1$_{Cr}$ variants [72]. A mutation at position G172$_{Cr}$ (corresponding to G302$_{Cp}$) towards aspartate in a double mutant with N267S$_{Cr}$ was shown to be four times as active as the wild type protein [72]. N267$_{Cr}$ lies in an external loop of the protein, while an aspartate at position 172/302 could bring additional electronegativity into the close proximity of the 4Fe$_H$-cluster. Thus the major part of the improvement might be attributed to G172D$_{Cr}$. The sequences examined in our alignment show an even distribution of G and A at the corresponding position (Fig. 3).

The adverse effects of changes in the direct interaction pattern between the polypeptide and the catalytic 2Fe$_H$ center demonstrate the enormous influence of the protein environment on stability and functionality of the H-cluster. Thus variation of less conserved amino acids seems more promising for future attempts to engineer [FeFe]-hydrogenases in the vicinity of the H-cluster. Research aiming at an increased oxygen tolerance could also profit from the improved understanding of the mechanism of O_2 induced inactivation. Modifying the H-cluster environment in a way either to block diffusion of ROS to the 4Fe$_H$-subcluster or to prevent the protonation of ROS has been suggested in this context [60,61].

5. Electron transfer

Mutagenesis in [FeFe]-hydrogenases is focused on modulating and characterizing structure function relationships within the H-domain. However, the potential influence of the electrochemical features of accessory clusters on catalytic behavior should not be neglected. H_2 oxidation and production are multistep processes and might well be limited by steps not involving the active site, but by H_2 transfer or electron transport [73,74].

First hints that accessory clusters influence the H-cluster performance emerged from one of the first publications about the effects of mutagenesis on [FeFe]-hydrogenase function [75]. The study characterized a pool of chimeric [FeFe]-hydrogenases obtained by molecular shuffling of the [FeFe]-hydrogenase genes of HydA$_{Ca}$ and HydA of *Clostridium sacharobutylicum* [75]. Among various active chimeric versions one exhibited a two fold increase in catalytic activity consisting of a fusion between the N-terminal part of HydA$_{Ca}$ and parts of the H-domain of HydA$_{Cs}$.

Recent examinations indeed implicate, that the function of accessory clusters in [FeFe]-hydrogenases goes beyond their assumed role of simple electron conducting centers. A significant difference in the behavior of the CO$_b$ ligand during catalysis was identified (Fig. 2), when comparing [FeFe]-hydrogenases of green algae that lack any accessory clusters with enzymes of a more complex domain organization (DdH D(M2), CpI (M3)) [14,56]. A transition of the bridging CO coordination to the terminal bound configuration might stabilize a low local redox potential at Fe$_d$. For green algal enzymes the bridging CO$_b$ coordination is characteristic for H$_{ox}$ and H$_{red}$ state and switches to the terminal coordination only in the most reduced H$_{sred}$ state. Enzymes that possess accessory clusters like DdH and HydA$_{Ca}$ however already exhibit the terminal CO$_b$ coordination in the H$_{red}$ state [14,16,76] indicating that the accessory clusters modulate or even buffer the redox potential at the 2Fe$_H$ site.

QM/MM calculations further confirm the influence of the accessory clusters on the electronic configuration of the H-cluster [74,77]. The states of the catalytic cycle were analyzed on the basis of a quantum mechanical model that includes beside the H-cluster both accessory cubane clusters (FS4A and FS4B; Fig. 1) of DdH (M2 type) [77]. The authors started the calculations with the Fe$_p$(I)Fe$_d$(II) state of the 2Fe$_H$-subcluster. Upon H_2 binding they determined a decrease in the energetic distance between the lowest unoccupied molecular orbital (LUMO) at the active site and the highest occupied molecular orbital (HOMO) at the distal F-cluster FS4B. The energetic barrier for electron transfer is further reduced when a positively charged redox partner binds at FS4B consequently triggering electron transfer and H_2 oxidation [77]. Interestingly, one electron reduction of the cluster assembly leads to reduction of FS4B and not of the H-cluster. A subsequent protonation of the 2Fe$_H$-subcluster induces electron transport back from FS4B to the active site [74].

According to these results, exchanges in the polypeptide ligand sphere of the accessory clusters should have an effect on its electrochemical features and thus on the redox behavior of the whole redox cofactor ensemble including the H-cluster. For [NiFe]-hydrogenases such an effect was determined after replacing the histidyl ligand of the distal cubane cluster by cystein. While proton transfer and protein stability were not affected the exchange caused a significant decrease in the electron transfer rates from and to this distal accessory cluster [78].

Interestingly, manipulation of the ligand sphere of the accessory clusters seems to influence the O_2 tolerance of [FeFe]-hydrogenases as well. In a random mutagenesis approach two positions in the immediate neighborhood of the proximal accessory cubane cluster in CpI were identified, whose modulation caused an enhancement of O_2 tolerance [79]. While several variants at position 197$_{Cp}$ lead to various levels of increased O_2-tolerance the exchange of position N160$_{Cp}$ to aspartic acid only provided additional tolerance when combined with the exchange I197V$_{Cp}$ [79]. Although a direct correlation seems unlikely, the co-localization of hot spots for the modulation of O_2 tolerance at the proximal accessory cluster resembles the recently determined strong influence of the proximal accessory cluster on oxygen sensitivity in O_2-tolerant [NiFe]-hydrogenases [80,81].

6. Photobiological H_2-production

Actual approaches for the design of photochemical H_2 production focus on electrochemically coupled systems of photosensitizer compounds and a H_2 producing catalytic center [18]. A natural blueprint for this concept is represented by the metabolic integration of [FeFe]-hydrogenases from green algae like *Chlamydomonas reinhardtii* [13,82–86]. Under anaerobiosis these [FeFe]-hydrogenases belong to a unique photofermentative H_2 metabolism that includes direct and indirect light dependent coupling of H_2O splitting and H_2 production [36,87,88]. HydA1$_{Cr}$ in *C. reinhardtii* functions as electron sink to dispose of excess redox power under these conditions by accepting electrons from the photosynthetic electron transport chain [36]. The photosynthetic ferredoxin PetF links not only the hydrogenase to photosynthesis, but allocates electrons also to a number of other redox-enzymes, most notably the FNR (ferredoxin:NADP$^+$-oxidoreductase) [89]. Thus, one key aspect for the efficient light driven H_2 production seems to be the interaction between PetF and the hydrogenase.

HydA1$_{Cr}$ exhibits a polar surface charge distribution (Fig. 4B) with an accumulation of 14 basic amino acid residues that cluster around the putative PetF binding site. At least eight among them are specifically conserved within the M1 group (Fig. 4A). A first site directed mutagenesis investigation focusing on ten surface positions showed that residues K396$_{Cr}$ and K433$_{Cr}$ play a major role for the electrostatic interactions driving and directing the electron transfer complex formation with PetF [89,90]. Current examinations further demonstrate that R227$_{Cr}$ is crucial for complex formation with PetF (Happe et al., unpublished data). While in M1-type [FeFe]-hydrogenases this arginine is strictly conserved, the general multiple sequence alignment demonstrates that for about 90% of the sequences alanine is identified at the corresponding position (Fig. 4A). This even includes the recently identified M3-type [FeFe]-hydrogenases of the trebouxiophycean alga *Chlorella variabilis* NC64A (Fig. 4), which is discussed as predecessor form of chlorophycean M1 type enzymes [91].

The potential to improve electron transfer efficiency between hydrogenase and ferredoxin has been proven by selectively exchanging amino acids with acidic or hydrophobic residues near and within the PetF binding site against lysine [92].

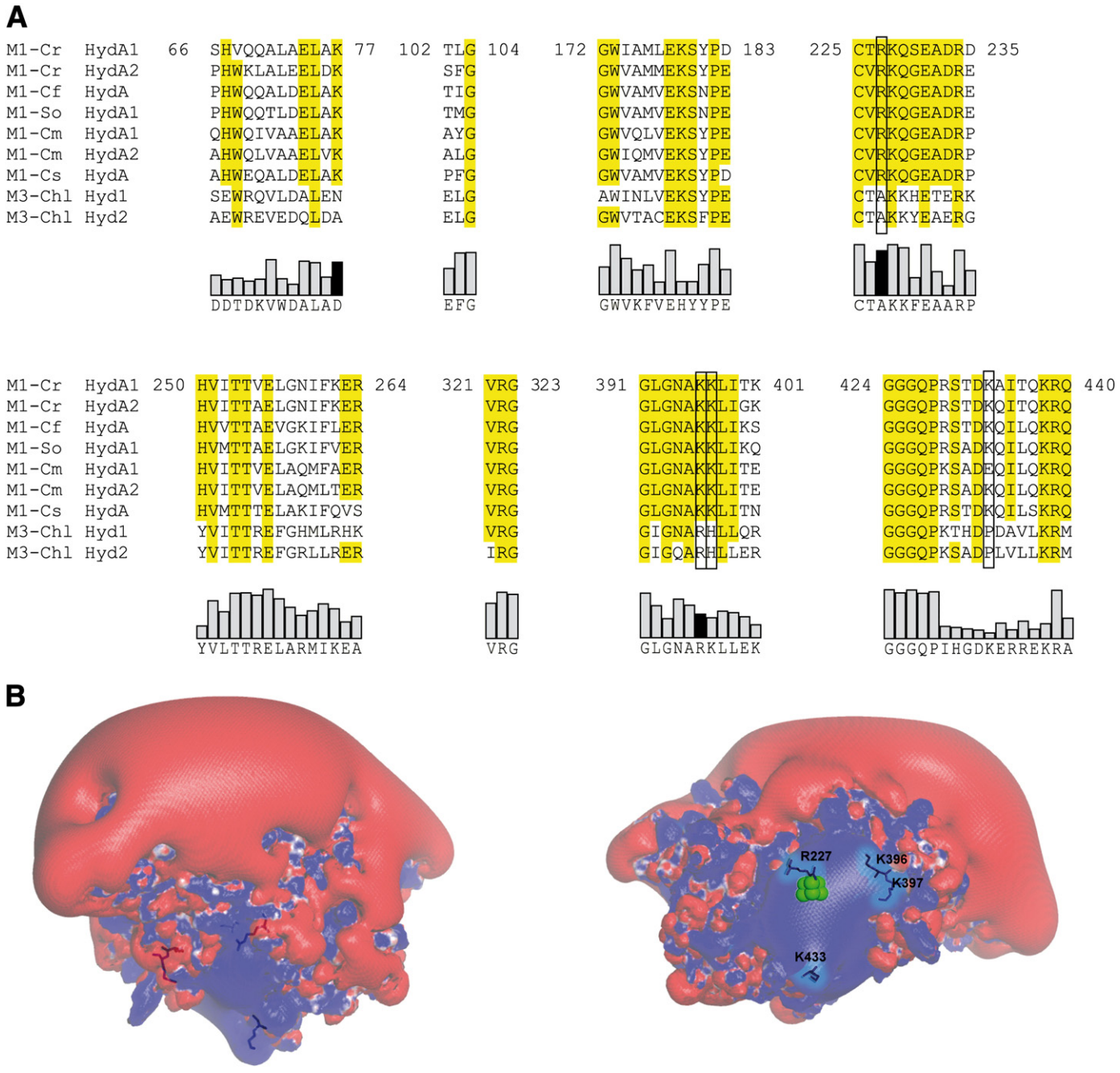

Fig. 4. Comparison of basic HydA residues necessary for complex formation with PetF. (A) Multiple sequence alignment that contains residues with relevance for PetF interaction and comprises selected [FeFe]-hydrogenases from different algal species. M1-Cr HydA1 and HydA2 (*C. reinhardtii*) [104], M1-Cf HydA (*Chlorella fusca*) [84], M1-So HydA1 (*Scenedemus obliquus*) [82], M1-Cm HydA1 and HydA2 (*Chlamydomonas moewusii*) [13], M1-Cs HydA (*Chlorococcum submarinum*) [13], M3-Chl Hyd1 and Hyd2 (*Chlorella variabilis* NC64A) [91]. A conservancy level above 75% is indicated by yellow background. Positions that dominantly determine the success of complex formation are marked by a frame. The relative conservancy levels of the entire multiple sequence alignment covering all [FeFe]-hydrogenase subgroups are presented below by grey columns. Black columns mark basic positions of M1-type enzymes that show a high conservation level in both alignments (identity ≥ 45%), but for a different amino acid. (B) Electrostatic surface charge distribution of $HydA1_{Cr}$ (PDB ID: 3LX4) calculated via the APBS tool of PyMOL according to Poisson–Boltzmann. Left: side view, right: bottom view on PetF interaction site near the H-cluster (green spheres) binding niche. Surface sections exhibiting a positive or negative net charge are shown in blue and red respectively. For the bottom view the locations of basic residues, that are involved in PetF interaction, are indicated by blue stick structures.

The authors further demonstrated that confined diffusion strategies, based on linker coupled chimeras between hydrogenase and electron mediator can improve electron transfer efficiency. When implementing the best linker length a fusion protein between $HydA_{Ca}$ and PetF from spinach exhibited a more than 4-fold higher PetF dependent H_2 production activity compared to separated proteins [92]. Similar fusion proteins between $HydA1_{Cr}$ and $PetF_{Cr}$ succeeded in limiting the competetive influence of the FNR on light dependent hydrogen production [93].

Another approach showed the possibility for a direct coupling of photosystem I (PSI) and hydrogenase [94]. The parallel exchange of the most exposed cysteine ligand of the respective distal accessory clusters in both the PSI subunit PsaC and $HydA_{Ca}$ to glycine allowed for the electrochemical wiring of the enzymes via their FeS clusters by a dithiolate linker compound. The resulting PSI/HydA construct enabled a sustained light driven H_2 production activity which even exceeded O_2 evolution efficiency during a time range of 90 days [94,95].

7. Transport channels

While electron transport is accomplished by an array of accessory clusters in the more diverse N- and C-terminal parts of [FeFe]-hydrogenases, passive transport of protons and small gas molecules like H_2, CO and O_2 to and from the active site occurs through the H-domain conserved in all types of [FeFe]-hydrogenases (Fig 5). Two pathways leading outward from a central cavity in CpI were identified by complementing a calculation of volumetric solvent accessibility with a molecular mechanics approach [96]. The central cavity is formed by nine strictly conserved residues (Fig. 5B, marked in red) and includes the open coordination site at Fe_d as a starting point of all channels. The conserved pathway A seems to be more rigid and corresponds to the "H_2-channel" earlier suggested according to the crystal structure data of DdH and CpI [5,7]. Along this channel H_2 diffusion can be simulated even for the static crystal structure in CpI [96]. Oxygen however can move along the pathway only by transient widening of the connections between cavities due to protein movement. Pathway B appears to be inaccessible for both H_2 and O_2 in the static crystal structure. MD simulations nevertheless indicate that it offers transient packing defects and connections between cavities for both H_2 and O_2 diffusion [96]. Generally the simulations indicate that O_2 moves stepwise from cavity to cavity along both major pathways.

Additional to pathways A and B, Lautier and coworkers list amino acids aligning a potential third pathway denoted as "wet channel" (pathway W), in which a trail of water molecules is present in the crystal structure of CpI [68]. This channel was discussed to be part of the proton transfer pathway, which is situated in close proximity [69].

The general features of the gas transfer system in [FeFe]-hydrogenases compare well to recent findings for the [NiFe]-hydrogenase from *Desulfovibrio fructosovorans* [97–99]. In both, CpI and *Df*[NiFe]-hydrogenase, gas diffusion to the active site seems not limited to one tunnel, but rather three putative pathways were identified. The additional pathways cannot be detected in the rigid protein structure or by Xe-binding experiments and have thus not been described in previous studies. Furthermore, movement along these pathways can be better described as hopping from one transient packing defect to the next heavily relying on side-chain fluctuations and even movement of the protein backbone. While H_2 seems to diffuse quickly through both proteins diffusion of O_2 is more limited and notably restricted at the active site [96,98].

Comparative protein film electrochemistry on the three different types of [FeFe]-hydrogenases confirmed the importance of the

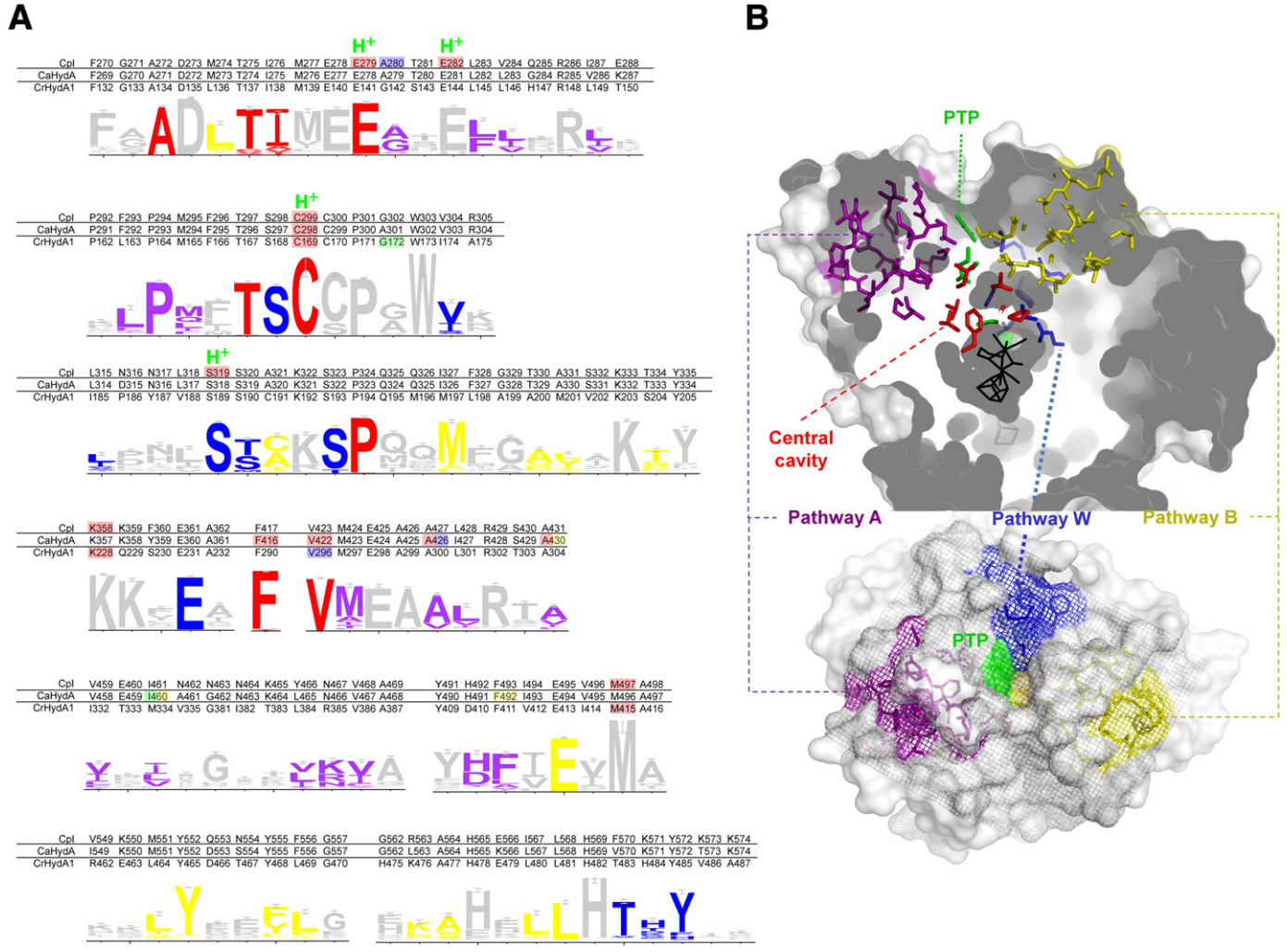

Fig. 5. Conserved substrate diffusion pathways through the H-domain of [FeFe]-hydrogenases. (A) Alignment of sequence regions of CpI, $HydA_{Ca}$ and $HydA1_{Cr}$ containing the putative pathways for substrate diffusion, the central cavity and the proposed proton transfer pathway. A sequence logo representation of a multiple sequence alignment of 828 sequences of [FeFe]-hydrogenases (see Table 1 and S1) is shown below and colored according to affiliation to the tunnels (color scheme as in B). Amino acids belonging to the proton transfer pathway are indicated above the alignment by a green H^+. Reported mutations with influence on activity or oxygen tolerance are marked by colored background as in Fig. 3B. (B) Cross section and top view on a surface representation of CpI (PDB ID: 3C8Y) with amino acids belonging to the substrate tunnels, the central cavity or the proton transfer pathway as stick models (colors as indicated) and the H-cluster represented by black lines.

protein framework for diffusion of CO and O_2 by showing significant differences in the diffusion rates for the three enzymes [58]. According to the second order rate constants for inhibition by CO and O_2, inhibition of DdH occurs 10-times faster compared to HydA1-$_{Cr}$ and by three orders of magnitude faster when compared to HydA$_{Ca}$ [58]. Furthermore, the results show that inactivation of DdH is limited by the redox state specific activity of the H-cluster rather than by diffusion velocity along the gas channel system. In contrast, for HydA$_{Ca}$ gas diffusion seems to be the limiting aspect for inhibition [58,100]. Taken together these findings implicate at least for some [FeFe]-hydrogenases the possibility to increase oxygen tolerance by narrowing the minimum diameter of the gas diffusion pathways. This could putatively lead to a molecular sieve effect, which selectively impedes diffusion of O_2 while still allowing efficient H_2 exchange. Focusing on HydA$_{Ca}$ Lautier and co-workers examined the effects of eight single amino acid exchanges generated with the intention either to block pathway A or the entrance to the central cavity [68]. The resulting variants were examined via isotope exchange assays and protein film electrochemistry allowing the determination of kinetic constants for the exchange of H_2, CO and O_2. Mutations at positions aligning the central cavity lead to a severe decrease of enzyme activity, which is not surprising given their high degree of conservation (Fig. 5). None of them increased O_2 tolerance significantly [68]. The other four examined amino acid exchanges were located further away from the active site. Among them only A426L$_{Ca}$ (427$_{Cp}$) was reported to reduce O_2 diffusion. Unfortunately, it also slows down H_2-diffusion and enzyme activity considerably.

Recently, variants with increased oxygen tolerance were found in a library of randomly mutated CpI proteins [79]. The authors reported that the exchange A280V$_{Cp}$, at a position belonging to pathway A, caused a slightly higher residual activity in combination with other structurally not related mutations. Though data about gas diffusion rates for variant A280V$_{Cp}$ are not available, it can be hypothesized that the increase in volume limits diffusion of O_2 through pathway A.

Even though blocking of transport channels has been a successful strategy for [NiFe]-hydrogenases [100–102], success with [FeFe]-hydrogenases has been so far rather limited. Calculations for the *Df*[NiFe]-hydrogenase indicate a minor role for the mean channel dia meter, but instead emphasize the role of gates, which need side chain fluctuations or backbone movements to let gas molecules diffuse from one cavity to the next [99]. Future attempts to increase oxygen tolerance by altering the gas diffusion pathways might need to identify similar gates and the corresponding movement nodes in [FeFe]-hydrogenases. The aim should be to limit these movements of the polypeptide by amino acid exchanges.

8. Perspectives and limits of mutagenesis

The wealth of information about the individual influences of single amino acids on the catalytic features demonstrates the value of effective expression systems in [FeFe]-hydrogenase research. However, maturation efficiencies and background activities often significantly deviate between different host systems and are hard to properly account for when discussing residual activities of variants.

Several examples discussed here further implicate that for most positions the effects of directed exchanges are hard to predict. Especially when prior experiments suggest an influential meaning it might be worth applying saturation mutagenesis for gaining deeper insights into the nature of the indicated influence as demonstrated by Bingham and coworkers REF [79] (Bingham et al., 2012). Rational approaches to locate positions that might have a positive influence on certain enzyme features, have limits due to the complexity of the interactions within a protein. As shown above, random strategies are not confined by these limits and can reveal more subtle but nonetheless valuable long range effects. However, purely random approaches like Error-Prone-PCR are restricted by time and financial aspects as they make it necessary to generate and screen a vast amount of variants. Therefore, future attempts to engineer [FeFe]-hydrogenases might either include concepts based more on selection or need intelligent compromises between a rational focus and random approaches.

The different functional units of the polypeptide clearly influence the reactivity and stability of the H-cluster itself. Some of these effects are long range effects, but still have a profound influence on the electrochemical configuration of the 2Fe$_H$-subcluster. Even though some of the effects might not be reproducible in H-cluster mimics, they should be seen as part of the natural model when designing synthetic compounds.

Supplementary data to this article can be found online at http://dx.doi.org/10.1016/j.bbabio.2013.03.004.

References

[1] M.T. Stiebritz, M. Reiher, A unifying structural and electronic concept for Hmd and [FeFe] hydrogenase active sites, Inorg. Chem. 49 (2010) 5818–5823.
[2] S. Shima, U. Ermler, Structure and function of [Fe]-hydrogenase and its iron–guanylylpyridinol (FeGP) cofactor, Eur. J. Inorg. Chem. 2011 (2011) 963–972.
[3] A. Volbeda, M.H. Charon, C. Piras, E.C. Hatchikian, M. Frey, J.C. Fontecilla-Camps, Crystal structure of the nickel–iron hydrogenase from *Desulfovibrio gigas*, Nature 373 (1995) 580–587.
[4] J.W. Peters, W.N. Lanzilotta, B.J. Lemon, L.C. Seefeldt, X-ray crystal structure of the Fe-only hydrogenase (CpI) from *Clostridium pasteurianum* to 1.8 angstrom resolution, Science 282 (1998) 1853–1858.
[5] Y. Nicolet, C. Piras, P. Legrand, C.E. Hatchikian, J.C. Fontecilla-Camps, *Desulfovibrio desulfuricans* iron hydrogenase: the structure shows unusual coordination to an active site Fe binuclear center, Structure 7 (1999) 13–23.
[6] M. Winkler, S. Kawelke, T. Happe, Light driven hydrogen production in protein based semi-artificial systems, Bioresour. Technol. 102 (2011) 8493–8500.
[7] Y. Nicolet, B.J. Lemon, J.C. Fontecilla-Camps, J.W. Peters, A novel FeS cluster in Fe-only hydrogenases, Trends Biochem. Sci. 25 (2000) 138–143.
[8] S.T. Stripp, G. Goldet, C. Brandmayr, O. Sanganas, K.A. Vincent, M. Haumann, F.A. Armstrong, T. Happe, How oxygen attacks [FeFe] hydrogenases from photosynthetic organisms, Proc. Natl. Acad. Sci. U. S. A. 106 (2009) 17331–17336.
[9] D.S. Patil, J.J. Moura, S.H. He, M. Teixeira, B.C. Prickril, D.V. DerVartanian, H.D. Peck, J. LeGall, B.H. Huynh, EPR-detectable redox centers of the periplasmic hydrogenase from *Desulfovibrio vulgaris*, J. Biol. Chem. 263 (1988) 18732–18738.
[10] A.J. Pierik, W.R. Hagen, J.S. Redeker, R.B.G. Wolbert, M. Boersma, M.F.J.M. Verhagen, H.J. Grande, C. Veeger, P.H.A. Mutsaers, R.H. Sands, W.R. Dunham, Redox properties of the iron–sulfur clusters in activated Fe-hydrogenase from *Desulfovibrio vulgaris* (Hildenborough), Eur. J. Biochem. 209 (1992) 63–72.
[11] A.S. Pereira, P. Tavares, I. Moura, J.J.G. Moura, B.H. Huynh, Mössbauer characterization of the iron–sulfur clusters in *Desulfovibrio vulgaris* hydrogenase, J. Am. Chem. Soc. 123 (2001) 2771–2782.
[12] W. Roseboom, A.L. Lacey, V.M. Fernandez, E.C. Hatchikian, S.P.J. Albracht, The active site of the [FeFe]-hydrogenase from *Desulfovibrio desulfuricans*. II. Redox properties, light sensitivity and CO-ligand exchange as observed by infrared spectroscopy, J. Biol. Inorg. Chem. 11 (2006) 102–118.
[13] C. Kamp, A. Silakov, M. Winkler, E.J. Reijerse, W. Lubitz, T. Happe, Isolation and first EPR characterization of the [FeFe]-hydrogenases from green algae, Biochim. Biophys. Acta 1777 (2008) 410–416.
[14] A. Silakov, C. Kamp, E. Reijerse, T. Happe, W. Lubitz, Spectroelectrochemical characterization of the active site of the [FeFe] hydrogenase HydA1 from *Chlamydomonas reinhardtii*, Biochemistry 48 (2009) 7780–7786.
[15] A. Silakov, B. Wenk, E. Reijerse, W. Lubitz, ^{14}N HYSCORE investigation of the H-cluster of [FeFe] hydrogenase: evidence for a nitrogen in the dithiol bridge, Phys. Chem. Chem. Phys. 11 (2009).
[16] Z. Chen, B.J. Lemon, S. Huang, D.J. Swartz, J.W. Peters, K.A. Bagley, Infrared studies of the CO-inhibited form of the Fe-only hydrogenase from *Clostridium pasteurianum* I: examination of its light sensitivity at cryogenic temperatures, Biochemistry 41 (2002) 2036–2043.
[17] C. Tard, X. Liu, S.K. Ibrahim, M. Bruschi, L. De Gioia, S.C. Davies, X. Yang, L.S. Wang, G. Sawers, C.J. Pickett, Synthesis of the H-cluster framework of iron-only hydrogenase, Nature 433 (2005) 610–613.
[18] M. Wang, L. Chen, X. Li, L. Sun, Approaches to efficient molecular catalyst systems for photochemical H2 production using [FeFe]-hydrogenase active site mimics, Dalton Trans. 40 (2011) 12793–12800.
[19] P.W. King, M.C. Posewitz, M.L. Ghirardi, M. Seibert, Functional studies of [FeFe] hydrogenase maturation in an *Escherichia coli* biosynthetic system, J. Bacteriol. 188 (2006) 2163–2172.
[20] D.W. Mulder, E.M. Shepard, J.E. Meuser, N. Joshi, P.W. King, M.C. Posewitz, J.B. Broderick, J.W. Peters, Insights into [FeFe]-hydrogenase structure, mechanism, and maturation, Structure 19 (2011) 1038–1052.
[21] M.C. Posewitz, P.W. King, S.L. Smolinski, L. Zhang, M. Seibert, M.L. Ghirardi, Discovery of two novel radical S-adenosylmethionine proteins required for the assembly of an active [Fe] hydrogenase, J. Biol. Chem. 279 (2004) 25711–25720.
[22] I. Czech, A. Silakov, W. Lubitz, T. Happe, The [FeFe]-hydrogenase maturase HydF from *Clostridium acetobutylicum* contains a CO and CN^- ligated iron cofactor, FEBS Lett. 584 (2010) 638–642.

[23] I. Czech, S. Stripp, O. Sanganas, N. Leidel, T. Happe, M. Haumann, The [FeFe]-hydrogenase maturation protein HydF contains a H-cluster like [4Fe4S]-2Fe site, FEBS Lett. 585 (2011) 225–230.
[24] Y. Nicolet, J.C. Fontecilla-Camps, Structure–function relationships in [FeFe]-hydrogenase active site maturation, J. Biol. Chem. 287 (2012) 13532–13540.
[25] L. Girbal, G. von Abendroth, M. Winkler, P.M.C. Benton, I. Meynial-Salles, C. Croux, J.W. Peters, T. Happe, P. Soucaille, Homologous and Heterologous Overexpression in Clostridium acetobutylicum and Characterization of Purified Clostridial and Algal Fe-Only Hydrogenases with High Specific Activities, Appl. Environ. Microbiol. 71 (5) (2005) 2777–2781, http://dx.doi.org/10.1128/aem.71.5.2777-2781.2005.
[26] G. von Abendroth, S. Stripp, A. Silakov, C. Croux, P. Soucaille, L. Girbal, T. Happe, Optimized over-expression of [FeFe] hydrogenases with high specific activity in *Clostridium acetobutylicum*, Int. J. Hydrog. Energy 33 (2008) 6076–6081.
[27] K. Sybirna, T. Antoine, P. Lindberg, V. Fourmond, M. Rousset, V. Mejean, H. Bottin, *Shewanella oneidensis*: a new and efficient system for expression and maturation of heterologous [Fe-Fe] hydrogenase from *Chlamydomonas reinhardtii*, BMC Biotechnol. 8 (2008) 73.
[28] J.M. Kuchenreuther, C.S. Grady-Smith, A.S. Bingham, S.J. George, S.P. Cramer, J.R. Swartz, High-yield expression of heterologous [FeFe] hydrogenases in *Escherichia coli*, PLoS One 5 (2010) e15491.
[29] I. Yacoby, L.T. Tegler, S. Pochekailov, S. Zhang, P.W. King, Optimized expression and purification for high-activity preparations of algal [FeFe]-hydrogenase, PLoS One 7 (2012) e35886.
[30] J. Meyer, [FeFe] hydrogenases and their evolution: a genomic perspective, Cell. Mol. Life Sci. 64 (2007) 1063–1084.
[31] A. Akhmanova, F. Voncken, T. van Alen, A. van Hoek, B. Boxma, G. Vogels, M. Veenhuis, J.H. Hackstein, A hydrogenosome with a genome, Nature 396 (1998) 527–528.
[32] F.G. Voncken, B. Boxma, A.H. van Hoek, A.S. Akhmanova, G.D. Vogels, M. Huynen, M. Veenhuis, J.H. Hackstein, A hydrogenosomal [Fe]-hydrogenase from the anaerobic chytrid *Neocallimastix* sp. L2, Gene 284 (2002) 103–112.
[33] D.G. Lindmark, M. Muller, Hydrogenosome, a cytoplasmic organelle of the anaerobic flagellate *Tritrichomonas foetus*, and its role in pyruvate metabolism, J. Biol. Chem. 248 (1973) 7724–7728.
[34] V.V. Emelyanov, A.V. Goldberg, Fermentation enzymes of *Giardia intestinalis*, pyruvate:ferredoxin oxidoreductase and hydrogenase, do not localize to its mitosomes, Microbiology 157 (2011) 1602–1611.
[35] D.S. Horner, P.G. Foster, T.M. Embley, Iron hydrogenases and the evolution of anaerobic eukaryotes, Mol. Biol. Evol. 17 (2000) 1695–1709.
[36] A. Hemschemeier, T. Happe, Alternative photosynthetic electron transport pathways during anaerobiosis in the green alga *Chlamydomonas reinhardtii*, Biochim. Biophys. Acta 1807 (2011) 919–926.
[37] P.M. Vignais, B. Billoud, Occurrence, classification, and biological function of hydrogenases: an overview, Chem. Rev. 107 (2007) 4206–4272.
[38] J. Balk, A.J. Pierik, D.J.A. Netz, U. Mühlenhoff, R. Lill, The hydrogenase-like Nar1p is essential for maturation of cytosolic and nuclear iron–sulphur proteins, EMBO J. 23 (2004) 2105–2115.
[39] R.M. Barton, H.J. Worman, Prenylated prelamin A interacts with Narf, a novel nuclear protein, J. Biol. Chem. 274 (1999) 30008–30018.
[40] D. Song, F.S. Lee, Mouse knock-out of IOP1 protein reveals its essential role in mammalian cytosolic iron–sulfur protein biogenesis, J. Biol. Chem. 286 (2011) 15797–15805.
[41] M. Fujii, N. Adachi, K. Shikatani, D. Ayusawa, [FeFe]-hydrogenase-like gene is involved in the regulation of sensitivity to oxygen in yeast and nematode, Genes Cells 14 (2009) 457–468.
[42] G.J. Schut, M.W.W. Adams, The iron-hydrogenase of *Thermotoga maritima* utilizes ferredoxin and NADH synergistically: a new perspective on anaerobic hydrogen production, J. Bacteriol. 191 (2009) 4451–4457.
[43] M. Calusinska, T. Happe, B. Joris, A. Wilmotte, The surprising diversity of clostridial hydrogenases: a comparative genomic perspective, Microbiology (Reading, Engl.) 156 (2010) 1575–1588.
[44] S.F. Altschul, W. Gish, W. Miller, E.W. Myers, D.J. Lipman, Basic local alignment search tool, J. Mol. Biol. 215 (1990) 403–410.
[45] R.C. Edgar, MUSCLE: multiple sequence alignment with high accuracy and high throughput, Nucleic Acids Res. 32 (2004) 1792–1797.
[46] A. Marchler-Bauer, S. Lu, J.B. Anderson, F. Chitsaz, M.K. Derbyshire, C. DeWeese-Scott, J.H. Fong, L.Y. Geer, R.C. Geer, N.R. Gonzales, M. Gwadz, D.I. Hurwitz, J.D. Jackson, Z. Ke, C.J. Lanczycki, F. Lu, G.H. Marchler, M. Mullokandov, M.V. Omelchenko, C.L. Robertson, J.S. Song, N. Thanki, R.A. Yamashita, D. Zhang, N. Zhang, C. Zheng, S.H. Bryant, CDD: a Conserved Domain Database for the functional annotation of proteins, Nucleic Acids Res. 39 (2011) D225–D229.
[47] A.S. Pandey, T.V. Harris, L.J. Giles, J.W. Peters, R.K. Szilagyi, Dithiomethylether as a ligand in the hydrogenase h-cluster, J. Am. Chem. Soc. 130 (2008) 4533–4540.
[48] B.J. Lemon, J.W. Peters, Binding of exogenously added carbon monoxide at the active site of the iron-only hydrogenase (CpI) from *Clostridium pasteurianum*, Biochemistry 38 (1999) 12969–12973.
[49] M. Bruschi, C. Greco, L. Bertini, P. Fantucci, U. Ryde, L.D. Gioia, Functionally relevant interplay between the Fe4S4 cluster and CN^- ligands in the active site of [FeFe]-hydrogenases, J. Am. Chem. Soc. 132 (2010) 4992–4993.
[50] Z.-P. Liu, P. Hu, A density functional theory study on the active center of Fe-only hydrogenase: characterization and electronic structure of the redox states, J. Am. Chem. Soc. 124 (2002) 5175–5182.
[51] J.W. Peters, W.N. Lanzilotta, B.J. Lemon, L.C. Seefeldt, X-ray crystal structure of the Fe-only hydrogenase (CpI) from *Clostridium pasteurianum* to 1.8 angstrom resolution, Science 282 (1998) 1853–1858.
[52] Y. Nicolet, A.L. de Lacey, X. Vernede, V.M. Fernandez, E.C. Hatchikian, J.C. Fontecilla-Camps, Crystallographic and FTIR spectroscopic evidence of changes in Fe coordination upon reduction of the active site of the Fe-only hydrogenase from *Desulfovibrio desulfuricans*, J. Am. Chem. Soc. 123 (2001) 1596–1601.
[53] A. Silakov, B. Wenk, E. Reijerse, W. Lubitz, (14)N HYSCORE investigation of the H-cluster of [FeFe] hydrogenase: evidence for a nitrogen in the dithiol bridge, Phys. Chem. Chem. Phys. 11 (2009) 6592–6599.
[54] A. Silakov, E.J. Reijerse, S.P.J. Albracht, E.C. Hatchikian, W. Lubitz, The electronic structure of the H-cluster in the [FeFe]-hydrogenase from *Desulfovibrio desulfuricans*: a Q-band 57Fe-ENDOR and HYSCORE study, J. Am. Chem. Soc. 129 (2007) 11447–11458.
[55] C.E. Foster, T. Krämer, A.F. Wait, A. Parkin, D.P. Jennings, T. Happe, J.E. McGrady, F.A. Armstrong, Inhibition of [FeFe]-hydrogenases by formaldehyde and wider mechanistic implications for biohydrogen activation, J. Am. Chem. Soc. 134 (2012) 7553–7557.
[56] A. Adamska, A. Silakov, C. Lambertz, O. Rüdiger, T. Happe, E. Reijerse, W. Lubitz, Identification and characterization of the "super-reduced" state of the H-cluster in [FeFe] hydrogenase: a new building block for the catalytic cycle? Angew. Chem. Int. Ed. (2012).
[57] M.W. Adams, The structure and mechanism of iron-hydrogenases, Biochim. Biophys. Acta 1020 (1990) 115–145.
[58] G. Goldet, C. Brandmayr, S.T. Stripp, T. Happe, C. Cavazza, J.C. Fontecilla-Camps, F.A. Armstrong, Electrochemical kinetic investigations of the reactions of [FeFe]-hydrogenases with carbon monoxide and oxygen: comparing the importance of gas tunnels and active-site electronic/redox effects, J. Am. Chem. Soc. 131 (2009) 14979–14989.
[59] A.F. Wait, C. Brandmayr, S.T. Stripp, C. Cavazza, J.C. Fontecilla-Camps, T. Happe, F.A. Armstrong, Formaldehyde—a rapid and reversible inhibitor of hydrogen production by [FeFe]-hydrogenases, J. Am. Chem. Soc. 133 (2011) 1282–1285.
[60] C. Lambertz, N. Leidel, K.G.V. Havelius, J. Noth, P. Chernev, M. Winkler, T. Happe, M. Haumann, O2 reactions at the six-iron active site (H-cluster) in [FeFe]-hydrogenase, J. Biol. Chem. 286 (2011) 40614–40623.
[61] M.K. Bruska, M.T. Stiebritz, M. Reiher, Regioselectivity of H cluster oxidation, J. Am. Chem. Soc. 133 (2011) 20588–20603.
[62] D.W. Mulder, E.S. Boyd, R. Sarma, R.K. Lange, J.A. Endrizzi, J.B. Broderick, J.W. Peters, Stepwise [FeFe]-hydrogenase H-cluster assembly revealed in the structure of HydA [Dgr] EFG, Nature 465 (2010) 248–251.
[63] M. Bruschi, C. Greco, M. Kaukonen, P. Fantucci, U. Ryde, L. De Gioia, Influence of the [2Fe]H subcluster environment on the properties of key intermediates in the catalytic cycle of [FeFe] hydrogenases: hints for the rational design of synthetic catalysts, Angew. Chem. Int. Ed. 48 (2009) 3503–3506.
[64] P. Knörzer, A. Silakov, C.E. Foster, F.A. Armstrong, W. Lubitz, T. Happe, Importance of the protein framework for catalytic activity of [FeFe]-hydrogenases, J. Biol. Chem. 287 (2012) 1489–1499.
[65] O.F. Erdem, L. Schwartz, M. Stein, A. Silakov, S. Kaur-Ghumaan, P. Huang, S. Ott, E.J. Reijerse, W. Lubitz, A model of the [FeFe] hydrogenase active site with a biologically relevant azadithiolate bridge: a spectroscopic and theoretical investigation, Angew. Chem. 50 (2011) 1439–1443.
[66] S.P.J. Albracht, W. Roseboom, E.C. Hatchikian, The active site of the [FeFe]-hydrogenase from *Desulfovibrio desulfuricans*. I. Light sensitivity and magnetic hyperfine interactions as observed by electron paramagnetic resonance, J. Biol. Inorg. Chem. 11 (2006) 88–101.
[67] Z. Cao, M.B. Hall, Modeling the active sites in metalloenzymes. 3. Density functional calculations on models for [Fe]-hydrogenase: structures and vibrational frequencies of the observed redox forms and the reaction mechanism at the diiron active center, J. Am. Chem. Soc. 123 (2001) 3734–3742.
[68] T. Lautier, P. Ezanno, C. Baffert, V. Fourmond, L. Cournac, J.C. Fontecilla-Camps, P. Soucaille, P. Bertrand, I. Meynial-Salles, C. Léger, The quest for a functional substrate access tunnel in FeFe hydrogenase, Faraday Discuss. 148 (2011) 385–407.
[69] A.J. Cornish, K. Gartner, H. Yang, J.W. Peters, E.L. Hegg, Mechanism of proton transfer in [FeFe]-hydrogenase from *Clostridium pasteurianum*, J. Biol. Chem. 286 (2011) 38341–38347.
[70] S. Morra, A. Giraudo, G. Di Nardo, P.W. King, G. Gilardi, F. Valetti, Site saturation mutagenesis demonstrates a central role for cysteine 298 as proton donor to the catalytic site in CaHydA [FeFe]-hydrogenase, PLoS One 7 (2012) e48400.
[71] G. Hong, A.J. Cornish, E.L. Hegg, R. Pachter, On understanding proton transfer to the biocatalytic [Fe–Fe]H sub-cluster in [Fe–Fe]H2ases: QM/MM MD simulations, Biochim. Biophys. Acta 1807 (2011) 510–517.
[72] J.A. Stapleton, J.R. Swartz, A cell-free microtiter plate screen for improved [FeFe] hydrogenases, PLoS One 5 (2010).
[73] A. Abou Hamdan, S. Dementin, P.-P. Liebgott, O. Gutierrez-Sanz, P. Richaud, A.L. De Lacey, M. Rousset, P. Bertrand, L. Cournac, C. Léger, Understanding and tuning the catalytic bias of hydrogenase, J. Am. Chem. Soc. (2012).
[74] C. Greco, M. Bruschi, P. Fantucci, U. Ryde, L. De Gioia, Probing the effects of one-electron reduction and protonation on the electronic properties of the Fe–S clusters in the active-ready form of [FeFe]-hydrogenases. A QM/MM investigation, Chemphyschem 12 (2011) 3376–3382.
[75] L.E. Nagy, J.E. Meuser, S. Plummer, M. Seibert, M.L. Ghirardi, P.W. King, D. Ahmann, M.C. Posewitz, Application of gene-shuffling for the rapid generation of novel [FeFe]-hydrogenase libraries, Biotechnol. Lett. 29 (2007) 421–430.
[76] T.M. Van Der Spek, A.F. Arendsen, R.P. Happe, S. Yun, K.A. Bagley, D.J. Stufkens, W.R. Hagen, S.P.J. Albracht, Similarities in the architecture of the active sites of Ni-hydrogenases and Fe-hydrogenases detected by means of infrared spectroscopy, Eur. J. Biochem. 237 (1996) 629–634.
[77] C. Greco, M. Bruschi, P. Fantucci, U. Ryde, L. De Gioia, Mechanistic and physiological implications of the interplay among iron–sulfur clusters in [FeFe]-hydrogenases. A QM/MM perspective, J. Am. Chem. Soc. 133 (2011) 18742–18749.

[78] S. Dementin, V. Belle, P. Bertrand, B. Guigliarelli, G. Adryanczyk-Perrier, A.L. De Lacey, V.M. Fernandez, M. Rousset, C. Leger, Changing the ligation of the distal [4Fe4S] cluster in NiFe hydrogenase impairs inter- and intramolecular electron transfers, J. Am. Chem. Soc. 128 (2006) 5209–5218.
[79] A.S. Bingham, P.R. Smith, J.R. Swartz, Evolution of an [FeFe] hydrogenase with decreased oxygen sensitivity, Int. J. Hydrog. Energy 37 (2012) 2965–2976.
[80] J. Fritsch, P. Scheerer, S. Frielingsdorf, S. Kroschinsky, B. Friedrich, O. Lenz, C.M.T. Spahn, The crystal structure of an oxygen-tolerant hydrogenase uncovers a novel iron–sulphur centre, Nature 479 (2011) 249–252.
[81] M.-E. Pandelia, W. Nitschke, P. Infossi, M.-T. Giudici-Orticoni, E. Bill, W. Lubitz, Characterization of a unique [FeS] cluster in the electron transfer chain of the oxygen tolerant [NiFe] hydrogenase from *Aquifex aeolicus*, Proc. Natl. Acad. Sci. 108 (2011) 6097–6102.
[82] L. Florin, A. Tsokoglou, T. Happe, A novel type of iron hydrogenase in the green alga *Scenedesmus obliquus* is linked to the photosynthetic electron transport chain, J. Biol. Chem. 276 (2001) 6125–6132.
[83] T. Happe, A. Kaminski, Differential regulation of the Fe-hydrogenase during anaerobic adaptation in the green alga *Chlamydomonas reinhardtii*, Eur. J. Biochem. 269 (2002) 1022–1032.
[84] M. Winkler, B. Heil, T. Happe, Isolation and molecular characterization of the [Fe]-hydrogenase from the unicellular green alga *Chlorella fusca*, Biochim. Biophys. Acta 1576 (2002) 330–334.
[85] M. Winkler, A. Hemschemeier, C. Gotor, A. Melis, T. Happe, [Fe]-hydrogenases in green algae: photo-fermentation and hydrogen evolution under sulfur deprivation, Int. J. Hydrog. Energy 27 (2002) 1431–1439.
[86] S.T. Stripp, T. Happe, How algae produce hydrogen—news from the photosynthetic hydrogenase, Dalton Trans. (2009) 9960–9969.
[87] A. Hemschemeier, S. Fouchard, L. Cournac, G. Peltier, T. Happe, Hydrogen production by *Chlamydomonas reinhardtii*: an elaborate interplay of electron sources and sinks, Planta 227 (2008) 397–407.
[88] A. Melis, T. Happe, Hydrogen production. Green algae as a source of energy, Plant Physiol. 127 (2001) 740–748.
[89] M. Winkler, A. Hemschemeier, J. Jacobs, S. Stripp, T. Happe, Multiple ferredoxin isoforms in *Chlamydomonas reinhardtii*—their role under stress conditions and biotechnological implications, Eur. J. Cell Biol. 89 (2010) 998–1004.
[90] M. Winkler, S. Kuhlgert, M. Hippler, T. Happe, Characterization of the key step for light-driven hydrogen evolution in green algae, J. Biol. Chem. 284 (2009) 36620–36627.
[91] J.E. Meuser, E.S. Boyd, G. Ananyev, D. Karns, R. Radakovits, U.M. Narayana Murthy, M.L. Ghirardi, G.C. Dismukes, J.W. Peters, M.C. Posewitz, Evolutionary significance of an algal gene encoding an [FeFe]-hydrogenase with F-domain homology and hydrogenase activity in *Chlorella variabilis* NC64A, Planta 234 (2011) 829–843.
[92] C.M. Agapakis, D.C. Ducat, P.M. Boyle, E.H. Wintermute, J.C. Way, P.A. Silver, Insulation of a synthetic hydrogen metabolism circuit in bacteria, J. Biol. Eng. 4 (2010).
[93] I. Yacoby, S. Pochekailov, H. Toporik, M.L. Ghirardi, P.W. King, S. Zhang, Photosynthetic electron partitioning between [FeFe]-hydrogenase and ferredoxin: $NADP^+$-oxidoreductase (FNR) enzymes in vitro, Proc. Natl. Acad. Sci. U. S. A. 108 (2011) 9396–9401.
[94] C.E. Lubner, P. Knörzer, P.J.N. Silva, K.A. Vincent, T. Happe, D.A. Bryant, J.H. Golbeck, Wiring an [FeFe]-hydrogenase with photosystem I for light-induced hydrogen production, Biochemistry 49 (2010) 10264–10266.
[95] C.E. Lubner, A.M. Applegate, P. Knörzer, A. Ganago, D.A. Bryant, T. Happe, J.H. Golbeck, Solar hydrogen-producing bionanodevice outperforms natural photosynthesis, Proc. Natl. Acad. Sci. U. S. A. 108 (2011) 20988–20991.
[96] J. Cohen, K. Kim, P. King, M. Seibert, K. Schulten, Finding gas diffusion pathways in proteins: application to O_2 and H_2 transport in CpI [FeFe]-hydrogenase and the role of packing defects, Structure 13 (2005) 1321–1329.
[97] P.-H. Wang, R.B. Best, J. Blumberger, A microscopic model for gas diffusion dynamics in a [NiFe]-hydrogenase, Phys. Chem. Chem. Phys. 13 (2011) 7708–7719.
[98] P.-H. Wang, R.B. Best, J. Blumberger, Multiscale simulation reveals multiple pathways for H_2 and O_2 transport in a [NiFe]-hydrogenase, J. Am. Chem. Soc. 133 (2011) 3548–3556.
[99] P.-H. Wang, J. Blumberger, Mechanistic insight into the blocking of CO diffusion in [NiFe]-hydrogenase mutants through multiscale simulation, Proc. Natl. Acad. Sci. (2012).
[100] P.-P. Liebgott, F. Leroux, B. Burlat, S. Dementin, C. Baffert, T. Lautier, V. Fourmond, P. Ceccaldi, C. Cavazza, I. Meynial-Salles, P. Soucaille, J.C. Fontecilla-Camps, B. Guigliarelli, P. Bertrand, M. Rousset, C. Léger, Relating diffusion along the substrate tunnel and oxygen sensitivity in hydrogenase, Nat. Chem. Biol. 6 (2010) 63–70.
[101] F. Leroux, S. Dementin, B. Burlat, L. Cournac, A. Volbeda, S. Champ, L. Martin, B. Guigliarelli, P. Bertrand, J. Fontecilla-Camps, M. Rousset, C. Léger, Experimental approaches to kinetics of gas diffusion in hydrogenase, Proc. Natl. Acad. Sci. 105 (2008) 11188–11193.
[102] S.b. Dementin, F. Leroux, L. Cournac, A.L.d. Lacey, A. Volbeda, C. Léger, B.n.d. Burlat, N. Martinez, S.p. Champ, L. Martin, O. Sanganas, M. Haumann, V.c.M. Fernández, B. Guigliarelli, J.C. Fontecilla-Camps, M. Rousset, Introduction of methionines in the gas channel makes [NiFe] hydrogenase aero-tolerant, J. Am. Chem. Soc. 131 (2009) 10156–10164.
[103] G.E. Crooks, G. Hon, J.M. Chandonia, S.E. Brenner, WebLogo: a sequence logo generator, Genome Res. 14 (2004) 1188–1190.
[104] M. Forestier, P. King, L. Zhang, M. Posewitz, S. Schwarzer, T. Happe, M.L. Ghirardi, M. Seibert, Expression of two [Fe]-hydrogenases in *Chlamydomonas reinhardtii* under anaerobic conditions, Eur. J. Biochem. 270 (2003) 2750–2758.